Predictive Control Considering Model Uncertainty for Variation Reduction in Multistage Assembly Processes

Jing Zhong, Jian Liu, and Jianjun Shi

***Abstract*—Active control for dimensional variation reduction in multistage assembly processes (MAPs) is a challenging issue for quality assurance. It is desirable to implement a system-level control strategy to minimize the end-of-line product variance, which is propagated from upstream manufacturing stages. Research has been conducted to realize such objective, based on the variation propagation models derived from the nominal parameters of product and process design. However, due to the uncertainties induced by the significant changes of process parameters, such designated model will be different from that of the actual process, and will not precisely represent the actual physics of the process. This model discrepancy may lead to the performance deterioration of the controllers. This paper proposed a feed-forward MAP control strategy that explicitly takes into account the uncertainties of model coefficients. The case study demonstrates that, when the model uncertainties are significant, the controller derived from the proposed approach outperforms that derived without considering the model uncertainty.**

***Note to Practitioners*—This paper was motivated by the development of the programmable toolings (PTs), which are increasingly used in multistage manufacturing processes. The PTs serve as tooling locators in a certain operation stage and can be programmed to adjust the parts and/or subassemblies positions to compensate the errors that have been introduced in the preceding stages. Therefore, the control of the PTs to make optimal adjustments is a challenging issue for the variation reduction purpose. The application of feed-forward control strategies based on variation propagation model can implement automatic adjustments on a part-by-part basis. However, due to the unavoidable random errors, the actual variation propagation model may randomly deviate from the nominal model derived according to the nominal product/process design parameters. The random errors may be introduced by the part fabrication process or by preceding assembly process. They may change the actual values of the model coefficients and cause the model uncertainty in practice. This type of model uncertainty may significantly deteriorate the performance of PTs when the magnitude of variation is large. This paper proposed an innovative control strategy taking into account the uncertainty of the variation propagation model. When the magnitude of process variation is large, the control action derived based on the proposed strategy will outperform that derived without considering model uncertainty. A case study is conducted to demonstrate its effectiveness.**

***Index Terms*—Model uncertainty, multistage assembly processes, predicative control, variation reduction.**

NOMENCLATURE:

N	number of stages in a MAP;
n_p	total number of parts to be assembled;
$LP_{1,i,k}$, $LP_{2,i,k}$	two locating points of part i at stage k ;
$LS_{1,s,k}$, $LS_{2,s,k}$	two locating points of subassembly s at stage k;
$SD_{i,k}\hat{SD}_{i,k}$, $\tilde{SD}_{s,k}$	the nominal, the true and the random deviation of the distance between the two locating points of part/subassembly i at stage k, respectively;
$\beta_{s,k}$, $\hat{\beta}_{s,k}$, $\tilde{\beta}_{s,k}$	the nominal, the true and the random deviation of the angle between the line linking $LS_{1,s,k}$ and $LS_{2,s,k}$ and the horizontal axis of the global coordinate system, respectively;
$\mathbf{x}_{i,k}$	the vector of dimensional deviation of part i at stage k;
$\mathbf{u}_k$	the vector of overall control actions taken at stage k;
$\mathbf{y}_k$	the vector of deviations of key product characteristics at stage k;
$\mathbf{M}$, $\hat{\mathbf{M}}$, $\tilde{\mathbf{M}}$	the nominal, the true and the random deviation of the matrix $\mathbf{M}$, respectively;
$\mathbf{A}_k$, $\mathbf{B}_k$, $\mathbf{C}_k$	system matrices of the state-space model;
$\mathbf{\Gamma}_k$, $\mathbf{\Psi}_k$	matrices depicting the relationship between final product quality and process inputs, which are the series product of $\mathbf{A}_k$, $\mathbf{B}_k$, and $\mathbf{C}_N$;
$\mathbf{Q}_N$, $\mathbf{R}_k$	weighting matrices in the optimization index;
J_k	optimization index at stage k.

Manuscript received May 01, 2009; revised August 24, 2009; accepted November 14, 2009. Date of publication January 15, 2010; date of current version October 06, 2010. This paper was recommended for publication by Associate Editor W. Cai and Editor M. Zhou upon evaluation of the reviewers' comments. This work was supported in part by the General Motors Collaborative Research Lab in Advance Vehicle Manufacturing at The University of Michigan. The authors also gratefully acknowledge the financial support from NSF Grant (CMMI–0927574).

J. Zhong is with Microsoft Corporation, Bellevue, WA 98004 USA (e-mail: jzhong@umich.edu).

J. Liu is with the Department of Systems and Industrial Engineering, University of Arizona, Tucson, AZ 85718 USA (e-mail: jianliu@sie.arizona.edu).

J. Shi is with the H. Milton Stewart School of Industrial and Systems Engineering, Georgia Institute of Technology, Atlanta, GA 30332 USA (e-mail: jianjun.shi@isye.gatech.edu).

Color versions of one or more of the figures in this paper are available online at http://ieeexplore.ieee.org.

Digital Object Identifier 10.1109/TASE.2009.2038714

I. Introduction

DIMENSIONAL variation reduction is a critical yet challenging problem in quality assurance of multistage assembly processes (MAPs). In MAPs, multiple operation stages are involved in generating designated Key Product Characteristics (KPCs) or functionality of a product. At a certain stage k, special causes, such as part fabrication error, fixture error, welding gun error, and robot positioning error, will increase the variation of some KPCs to a level that exceeds their specification limits. In conjunction with the input quality transmitted from preceding stages, these quality problems will be further propagated to the downstream stages and accumulated to the final product. This variation propagation makes the variation reduction for MAPs especially challenging.

In order to improve the process stability and reduce the product variation, three types of approaches are widely adopted in practice: i) robust process design, which aims to reduce the impact of variation sources at the product and/or process design phase, such as robust locator pin layout design [1]; ii) Statistical Process Control (SPC), which detects process parameter changes from quality measurements of KPCs; and iii) in-process active control, which compensates the error based on in-process measurements. Among them, robust design is usually conducted in the design phase of product realization and will not react to in-process disturbances. SPC focuses mainly on fault detection, rather than process adjustment, and in-process control actively corrects deviation of each assembly, and can thus achieve variation reduction on a part-by-part base.

The application of in-process control in MAPs is complex, in the sense that variation is propagated and accumulated throughout the production line. Therefore, a successful control strategy for MAPs should systematically compensates error at an intermediate stage with the aim to achieve the overall best quality at the final stage, rather than the best quality at an intermediate stage where the control action is taken. In other words, the system-level optimal, not the stage-level optimal, should be the control objective.

In-process control for MAPs has received intensive study and promising results have been reported in literatures. An optimal control scheme was proposed for mechanical assembly process using state transition models [2]. This approach treats control as stochastic discrete-time linear optimal regulator problem, and obtains a deterministic controller with parts considered as the only source of variation in the process. A similar optimal control problem is analyzed, for the application in semiconductor manufacturing [3]. The authors used Dynamic Programming (DP) as the optimization tool. The decision variables include the control magnitudes in every direction on every individual part, and controllable environmental variables in an individual manufacturing stage.

Variation reduction using feedback control requires the existence of autocorrelation in the variation sources. However, in the discrete part multistage manufacturing processes, the process induced variations will be different from part/subassembly to part/subassembly, the autocorrelation does not exist or is very weak [4], [5]. As the control actions taken to compensate deviations are in a part-by-part manner, the control actions executed on the current part/subassembly would be based on the deviation measurements collected from the previous part/subassembly if a feedback control strategy was adopted. For instance, a dimensional deviation is observed on part A and the control action can be derived based on the observed deviations, which reflect the magnitudes of process deviations affecting part A at that particular time. However, when the control action is taken, the magnitudes of process deviations affecting another part, say part B, has already been different. With the absence of autocorrelations, such control actions would not be effective and might lead to overcontrol actions and thus even increase process variations.

The use of feed-forward control strategies, through adjustments or reconfigurations of tools and fixtures, has shown a promising future in improving final product quality of multistage machining processes [6], [7] and MAPs [8], [9]. These feed-forward control strategies are implemented through the integration of in-line measurements, programmable toolings (PTs) and variation propagation models, which mathematically describe the induction, transition and accumulation of random process errors along process stages. A fundamental assumption for these studies is that the underlying variation propagation model used for deriving the control action is precise and accurate. However, the models used in designing the control actions are typically obtained from the nominal product and process design information. In practice, there are unavoidable random errors that lead to the random deviations of the actual model from the nominal model. This type of model uncertainties may generate negative impacts on the control performance.

The problem of model uncertainty has drawn much attention in the system and control community. In control systems, due to the imperfect data, limited process knowledge and complex system dynamics, models of the system to be controlled always have inherent errors. Different control methodologies have been developed to address the issue of model uncertainty, such as Model Reference Adaptive Control (MRAC), H_∞ control [10]–[12], and Fuzzy Control [13], which is capable of controlling a system without the complex mathematical modeling. However, due to the difference between the dynamic model for system control and the variation propagation model for variation reduction, such methodologies cannot be directly applied to the control of MAPs.

In this paper, a feed-forward predictive control methodology with considering model uncertainty is developed to optimally determine the control action. To the best of our knowledge, it is the first methodology that explicitly takes into account the model uncertainty to optimally reduce the KPC's dimensional variation of MAPs. This problem will be investigated with two steps: (i) improving the variation propagation modeling methods by incorporating the variations introduced by incoming parts or subassemblies in the model and (ii) developing a predictive control approach to deriving the control actions of one PT installed in an intermediate stage of a MAP. The proposed research deals with MAPs where control is performed on one out of all the stages. The control strategy for multiple controllable stages is not a simple addition of this single control situation, because the control taken in later stages may interfere with the result of the action performed in previous stages. The extension to multiple control stages can be a future direction

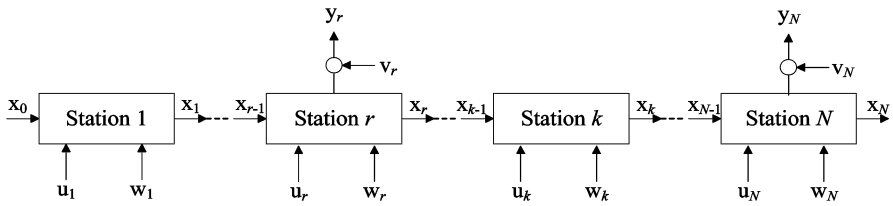

Fig. 1. Illustration of variation propagation in a MAP.

of the research. The rest of this paper is organized as follows: Section II introduces the extension of the state-space model to explicitly represent potential model uncertainty. Section III derives predictive control strategy based on this model considering uncertainties. Section IV demonstrates the effectiveness of the proposed method with a case study motivated by a real-life assembly process. Concluding remarks can be found in Section V.

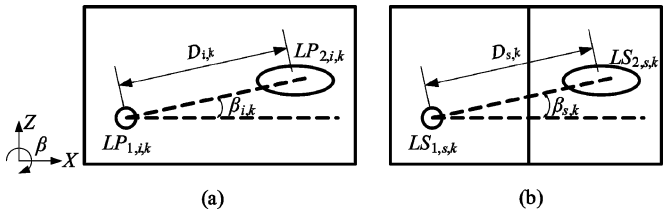

Fig. 2. Representation of part deviation. (a) Single Part. (b) Subassembly.

II. State-Space Modeling and Model Uncertainty

The variation propagation in a MAP can be illustrated by Fig. 1. Parts from suppliers enter the production at stage 1 with initial fabrication errors, denoted as $\mathbf{x}_0$. At stage 1, the part control action, denoted as $\mathbf{u}_1$, is applied through PT first, while other unmodeled process errors, such as process background disturbances, denoted as $\mathbf{w}_1$, are also introduced to the process. The designed operation at stage 1 is performed and variations on the subassembly will present, denoted as $\mathbf{x}_1$. This subassembly is then transferred to the next stage, and such variations propagate and accumulate similarly as more parts/subassemblies are joined together, until the whole assembly exits the production line from the final stage, stage N. The KPCs will be measured at stage N as well as some intermediate stages such as stage k, denoted as $\mathbf{y}_k$. Due to the imperfection of the measuring devices, measurement error, denoted as $\mathbf{v}_k$, will also be introduced to $\mathbf{y}_k$.

This type of variation propagation can be represented mathematically by a state-space model [14], [15]. When the model uncertainty is not explicitly considered, the model is defined as

$$\begin{cases} \mathbf{x}_k = \mathbf{A}_{k-1}\mathbf{x}_{k-1} + \mathbf{B}_k\mathbf{u}_k + \mathbf{w}_k \\ \mathbf{y}_k = \mathbf{C}_k\mathbf{x}_k + \mathbf{v}_k \end{cases}, \quad k = 1, \ldots, N. \quad (1)$$

The first equation is a state transition equation, where $\mathbf{x}$, $\mathbf{x}_k \in \mathbf{R}^{n\times 1}$, represents the deviations of quality features at stage k and n is the number of quality features considered in $\mathbf{x}_k$. Matrix $\mathbf{A}_k$, $\mathbf{A}_k \in \mathbf{R}^{n\times n}$, is the reorientation matrix that describes the error transferred from previous stage through part reorientation. Matrix $\mathbf{B}_k$, $\mathbf{B}_k \in \mathbf{R}^{n\times p}$, describes the impact of the PT control actions on $\mathbf{x}_k$. The second equation is an observation equation, where matrix $\mathbf{C}_k$, $\mathbf{C}_k \in \mathbf{R}^{m\times n}$, represents how the deviations of quality features are transformed to the deviations of KPC measurements denoted by $\mathbf{y}_N$, $\mathbf{y}_k \in \mathbf{R}^{m\times 1}$. The un-modeled disturbance and the measurement errors are denoted as $\mathbf{w}_k$ and $\mathbf{v}_k$, respectively, and $\mathbf{w}_k \in \mathbf{R}^{n\times 1}$ and $\mathbf{v}_k \in \mathbf{R}^{m\times 1}$.

Modeling variation propagation in a MAP is a procedure of deriving the model coefficient matrices, $\mathbf{A}_k$'s, $\mathbf{B}_k$'s, and $\mathbf{C}_k$'s. This is done by representing and investigating random deviations of features and parts with respect to different coordinate systems (CSs), based on the given product and process design information [14], [16].

A. Representation of Part Deviations and Model Uncertainty

Two types of CSs are used to properly represent parts' deviations, namely, global (or body) CS and part CS. The global CS remains unchanged for all stages, and part CS is attached onto a particular part or a subassembly. Each part is characterized by its deviation from the nominal position. In automotive body assembly process, the deviations of sheet metal assembly can be simplified into a 2-D case if parts are joined on slip planes [16]. Thus, the deviations can be represented by two translational coordinates, X and Z, and one rotational coordinates, β, as shown in Fig. 2. The subscript (i, k) in Fig. 2(a) indicates that the coordinate variables are for part i located at stage k, where $i = 1, \ldots, n_p$, $k = 1, \ldots, N$, and n_p is the total number of parts, and N is the total number of stages in a MAP. When a subassembly that consists of multiple parts is located, the subscript becomes (s, k) with s, $s = 1, \ldots, S_k$, denoting the index of subassembly, where S_k is the number of subassemblies to be assembled at stage k.

In a 2-D rigid part assembly process, a four-way hole and a two-way slot that are usually used to locate a part or a subassembly. The center of the hole and the center of the slot are chosen as the reference points, which are used to represent a part coordinate system in a 2-D space. These two points are denoted as $LP_{1,i,k}$ and $LP_{2,i,k}$ for a part, and as $LS_{1,s,k}$ and $LS_{2,s,k}$ for a subassembly. The position of a subassembly at stage k can then be represented by the position of $LS_{1,s,k}$, i.e., $(LS_{1,s,k}(x), LS_{1,s,k}(z))$ in the global coordinate system, and the angle, $\beta_{s,k}$, between the line connecting $LS_{1,s,k}$ and $LS_{2,s,k}$ and the x axis of global coordinate system, as shown in Fig. 2(b).

Under ideal production conditions, parts are located in their nominal positions, without fixture variations or part variations. However, in real production, locating tools and/or part features are not perfect. This imperfection will make the parts or subassemblies deviate from their nominal positions. Instead of directly using the global coordinates, the actual position of part in

space is described by its deviations from the nominal positions, i.e.,

$$\mathbf{x}_{i,k} = [\,\delta x_{i,k} \quad \delta z_{i,k} \quad \delta\beta_{i,k}\,]^T. \tag{2}$$

$\mathbf{x}_{i,k}$ denotes the random deviations with respect to the three coordinates (X, Z and β) of part i at stage k. For all the n_p parts assembled in a MAP, the deviations of the whole assembly on stage k can be defined as

$$\mathbf{x}_k = \left[\,\mathbf{x}_{1,k}^T \quad \cdots \quad \mathbf{x}_{n_p,k}^T\,\right]^T \tag{3}$$

which is the state vector of the model. If part i has not yet appeared at stage k, the corresponding $\mathbf{x}_{i,k} = \mathbf{0}$. With the same definition scheme, the deviations of a subassembly at stage k of a MAP is defined as $\mathbf{q}_{s,k}$, where

$$\mathbf{q}_{s,k} = [\,\delta x_{s,k} \quad \delta z_{s,k} \quad \delta\beta_{s,k}\,]^T. \tag{4}$$

At an assembly stage with PTs, parts or subassemblies are located by the actuators, such as PTs. The actuator that control the location of subassembly s is defined as (5) shown at the bottom of the page, where an element of $\mathbf{u}_{s,k}$ represents the adjustment of a reference point ($LS_{1,s,k}$ or $LS_{2,s,k}$) along a coordinate (x or z). Based on this definition, the actuator control action vector at stage k, $\mathbf{u}_k$, can be denoted as

$$\mathbf{u}_k \equiv \left[\,\mathbf{u}_{1,k}^T \quad \cdots \quad \mathbf{u}_{n_k,k}^T\,\right]^T \tag{6}$$

which contains the control actions of all the actuators of the n_k locator pairs used at stage k. In this paper, $\mathbf{u}_k$ represents the PT control actions only. It is true that these actions may also introduce variations into the process due to the controller variability, but it is also reasonable to ignore such variations in this research frame. Using superscript "^{C}" to represent the control action calculated by control law, and superscript "^{F}" to represent the actuator errors, the state transition equation can be further represented as $\mathbf{x}_k = \mathbf{A}_{k-1}\mathbf{x}_{k-1} + \mathbf{B}_k^C\mathbf{u}^C + \mathbf{B}_k^F\mathbf{u}^F + \mathbf{w}_k$, where $\mathbf{u}^F$ represents the random deviations induced by controller variability. However, these deviations are comparatively very small since the PTs employed in current MAPs are with high precision [17]. It provides some confidence on the precision. For example, the repeatability of Fanuc robot F-200iB is ± 0.1 mm, which is significantly smaller than the control magnitude. In this situation, the magnitude of $\mathbf{u}^C$ is significantly larger than $\mathbf{u}^F$, and thus the third term can be neglected.

The general state-space modeling procedures discussed in literatures [14] and [15] assume that the model coefficients are constants. However, in real production, the unavoidable process errors and parts imperfections will cause the random deviations of those model coefficients. This type of model uncertainty will deteriorate the performance of the control actions derived based on the nominal model. In this paper, model uncertainties will be explicitly considered in deriving the state-space model. New notations will be introduced to differentiate the designated process models and their true counterparts. A coefficient matrix with a "$\widehat{\ }$" is with true process parameters, whereas a matrix with a "$\sim$" is the deviation of the corresponding true matrix from its nominal matrix, e.g., $\widehat{\mathbf{M}} = \mathbf{M} + \tilde{\mathbf{M}}$. A matrix without a superscript is the nominal matrix derived from design parameters. With this notation scheme, two lemmas can be proposed based on the model derivation in [15].

Lemma 1: If subassembly s at stage k is located at points $LS_{1,s,k}$ and $LS_{2,s,k}$, then its deviations due to small deviations of the locators can be derived as

$$\mathbf{q}_{s,k} = \widehat{\mathbf{T}}_1^{s,k}\begin{bmatrix}\delta LS_{1,s,k}(x)\\ \delta LS_{1,s,k}(z)\\ \delta LS_{2,s,k}(x)\\ \delta LS_{2,s,k}(z)\end{bmatrix} = \widehat{\mathbf{T}}_1^{s,k}\cdot\mathbf{u}_{s,k} \tag{7}$$

where

$$\begin{aligned}\widehat{\mathbf{T}}_1^{s,k} &= \begin{bmatrix} 1 & 0 & 0 & 0\\ 0 & 1 & 0 & 0\\ \frac{\sin\widehat{\beta}_{s,k}}{\widehat{D}_{s,k}} & -\frac{\cos\widehat{\beta}_{s,k}}{\widehat{D}_{s,k}} & -\frac{\sin\widehat{\beta}_{s,k}}{\widehat{D}_{s,k}} & \frac{\cos\widehat{\beta}_{s,k}}{\widehat{D}_{s,k}}\end{bmatrix}\\ &= \mathbf{T}_1^{s,k} + \tilde{\mathbf{T}}_1^{s,k}.\end{aligned} \tag{8}$$

$\widehat{D}_{s,k}$ is the true distance between $LS_{1,s,k}$ and $LS_{2,s,k}$, where $\widehat{D}_{s,k} = D_{s,k} + \tilde{D}_{s,k}$, and $\tilde{D}_{s,k}$ represents the random dimensional deviation of the distance between the two locating holes. $\widehat{\beta}_{s,k}$ is the true angle between the line linking $LS_{1,s,k}$ and $LS_{2,s,k}$ and the horizontal axis of the global coordinate system.

The next lemma characterizes the reorientation operation, which induces deviations on parts when a subassembly is transferred from a preceding stage, even if the locating points in the current stage are free of error.

Lemma 2: Suppose that subassembly s is located at $LS_{1,s,k}$ and $LS_{2,s,k}$ at stage k and these two locating points are free of error, the deviations of subassembly s, when it is transferred from stage $k-1$ to stage k, can be calculated by a linear combination of deviations accumulated in its locating points, $LS_{1,s,k}$ and $LS_{2,s,k}$, at the previous stage $k-1$

$$\mathbf{q}_{s,k} = \widehat{\mathbf{T}}_2^{k-1,k}\begin{bmatrix}\delta LS_{1,s,k-1}(x)\\ \delta LS_{1,s,k-1}(z)\\ \delta LS_{2,s,k-1}(x)\\ \delta LS_{2,s,k-1}(z)\end{bmatrix} \tag{9}$$

where

$$\begin{aligned}\widehat{\mathbf{T}}_2^{k-1,k} &= \begin{bmatrix} -1 & 0 & 0 & 0\\ 0 & -1 & 0 & 0\\ -\frac{\sin\widehat{\beta}_{s,k}}{\widehat{D}_{s,k}} & \frac{\cos\widehat{\beta}_{s,k}}{\widehat{D}_{s,k}} & \frac{\sin\widehat{\beta}_{s,k}}{\widehat{D}_{s,k}} & -\frac{\cos\widehat{\beta}_{s,k}}{\widehat{D}_{s,k}}\end{bmatrix}\\ &= \mathbf{T}_2^{k-1,k} + \tilde{\mathbf{T}}_2^{k-1,k}.\end{aligned} \tag{10}$$

$$\mathbf{u}_{s,k} = [\,\delta u_{LS_{1,s,k}}(x) \quad \delta u_{LS_{1,s,k}}(z) \quad \delta u_{LS_{2,s,k}}(x) \quad \delta u_{LS_{2,s,k}}(z)\,]^T \tag{5}$$

The above two lemmas will be used to derive the state-space model with consideration of the uncertainties induced by random process errors.

B. State Space Model With Part Induced Uncertainty

As aforementioned, the random process deviations will not only appear as part errors in state vector $\mathbf{x}_k$ as considered in literatures, but also change the system matrices derived from the nominal design parameters, leading to the unavoidable model uncertainties. And the uncertainty of the system matrices, $\tilde{\mathbf{A}}_k$ and $\tilde{\mathbf{B}}_k$, can be introduced by dimensional variations of part features. For instance, the term $\tilde{\mathbf{T}}_1^{s,k}$ in (7) is determined by the dimensional variation of the distance between the two locating holes, i.e., $\hat{D}_{s,k}$. The magnitudes of the uncertainty of the system matrices can be estimated based on the standard deviation of part features, σ_I, which may come from the tolerance specifications provided by suppliers. This σ_I will be used to derive/estimate the mean vector and variance/covariance matrix of the system matrices. With the same notation mechanism used in (1), the state-space model can be reformulated as

$$\begin{cases} \mathbf{x}_k = \hat{\mathbf{A}}_{k-1}\mathbf{x}_{k-1} + \hat{\mathbf{B}}_k\mathbf{u}_k + \mathbf{w}_k \\ \mathbf{y}_k = \mathbf{C}_k\mathbf{x}_k + \mathbf{v}_k, \end{cases}, \quad k = 1, \ldots, N \tag{11}$$

where

$$\hat{\mathbf{A}}_k = \mathbf{A}_k + \tilde{\mathbf{A}}_k \text{ and } \hat{\mathbf{B}}_k = \mathbf{B}_k + \tilde{\mathbf{B}}_k. \tag{12}$$

$\hat{\mathbf{A}}_k$ and $\hat{\mathbf{B}}_k$ denote the true system matrices, whose coefficients randomly deviate from that of the nominal matrices, $\mathbf{A}_k$ and $\mathbf{B}_k$, by $\tilde{\mathbf{A}}_k$ and $\tilde{\mathbf{B}}_k$, respectively. Observation matrix $\mathbf{C}_k$ is considered as a constant matrix, which means the locating points are monitored directly and precisely.

The coefficient matrices $\hat{\mathbf{A}}_k$, $\hat{\mathbf{B}}_k$ and $\mathbf{C}_k$ are derived according to the given product and process design information, with consideration of model uncertainty. Following the modeling method in [15] and [16], these matrices are functions of $\hat{\mathbf{T}}_1^{s,k}$ and $\hat{\mathbf{T}}_2^{k-1,k}$ defined in Lemmas 1 and 2, respectively. A state transition matrix

$$\hat{\mathbf{\Phi}}_{k,i} = \hat{\mathbf{A}}_{k-1}\hat{\mathbf{A}}_{k-2}\ldots\hat{\mathbf{A}}_i, \quad k > i \tag{13}$$

is defined to model the deviation transition between stage i and k, where $i = k$, and $\hat{\mathbf{\Phi}}_{i,i} = \mathbf{I}_{n\times n}$, where $\mathbf{I}_{n\times n}$ is an identity matrix. Thus, the model (11) can be written in an input-output form as

$$\mathbf{y}_N = \sum_{i=1}^{N}\hat{\mathbf{\Gamma}}_i\mathbf{u}_i + \hat{\mathbf{\Gamma}}_0\mathbf{x}_0 + \sum_{i=1}^{N}\hat{\mathbf{\Psi}}_i\mathbf{w}_i + \mathbf{v}_N \tag{14}$$

where

$$\hat{\mathbf{\Gamma}}_i = \mathbf{\Gamma}_i + \tilde{\mathbf{\Gamma}}_i = \mathbf{C}_N\hat{\mathbf{\Phi}}_{N,i}\hat{\mathbf{B}}_i, \quad \hat{\mathbf{\Gamma}}_0 = \mathbf{C}_N\hat{\mathbf{\Phi}}_{N,0} \tag{15}$$

and

$$\hat{\mathbf{\Psi}}_i = \mathbf{\Psi}_i + \tilde{\mathbf{\Psi}}_i = \mathbf{C}_N\hat{\mathbf{\Phi}}_{N,i}. \tag{16}$$

It is assumed that if measurements taken at stage r, $\mathbf{y}_r$, is known, $\mathbf{x}_r$ can be obtained through the inverse of observation equation in (11), as $\hat{\mathbf{x}}_r = \mathbf{C}^{\dagger}\mathbf{y}_r$, where "$\mathbf{M}^{\dagger}$" represents a generalized inverse of matrix $\mathbf{M}$. Based on $\hat{\mathbf{x}}_r$, the final deviations of KPC measurements (collected at stage N) at stage k is estimated as

$$\begin{aligned}\hat{\mathbf{y}}_{N|k} &= \sum_{i=k}^{N}\hat{\mathbf{\Gamma}}_i\mathbf{u}_i + \hat{\mathbf{\Psi}}_r\hat{\mathbf{x}}_r + \sum_{i=r+1}^{N}\hat{\mathbf{\Psi}}_i\mathbf{w}_i + \mathbf{v}_N \\ &= \hat{\mathbf{\Gamma}}_k\mathbf{u}_k + \hat{\mathbf{\Psi}}_r\hat{\mathbf{x}}_r + \sum_{i=r+1}^{N}\hat{\mathbf{\Psi}}_i\mathbf{w}_i + \mathbf{v}_N. \end{aligned} \tag{17}$$

In this paper, we consider the scenario that one actuator installed at an intermediate stage, stage k, of a MAP. Thus, the term $\sum_{i=k}^{N}\hat{\mathbf{\Gamma}}_i\mathbf{u}_i$ in (14) is reduced to $\mathbf{\Gamma}_k\mathbf{u}_k$. It should also be noted that the sensors are not necessarily to be installed at the same stage as the actuators. This formulation relaxes the requirements proposed in previous works [8]. By using (11) through (17), the model uncertainty can be explicitly considered in control algorithm development.

III. Feed-Forward Predictive Control With Considering Model Uncertainty

At stage k of a MAP with control capability, the measurements of the deviations that have already been built into the parts and/or subassemblies will be the inputs to the predictive controller. These inputs are achieved from the measurements collected in a preceding assembly stage. The controller then decides the control action based on these measurements. In this paper, it is assumed that the control actions are performed by a controller that is installed in one given intermediate stage. This controller is called model predictive controller because it is designed based on the variation of KPCs at the final stage, predicted by the state-space model.

This section proposes a predictive control strategy using the state-space model with uncertainty. The decision of control action is formulated as an optimization problem with objective set to minimize the expectation of the quadratic form of the final product quality and that of the control cost.

A. Optimization Index of the Model Predictive Control (MPC)

Model predictive control (MPC) refers to computer control algorithms that utilize an explicit process model to predict the future response of a process [18]. The controller employed can be any control algorithms, such as Linear-Quadratic-Gaussian (LQG), and common model forms such as input-output (IO), first-principles (FP), that are widely used in linear and nonlinear systems [19]. MPC has been widely used in applications such as chemicals processes [20], mining processes, and automotive actuator design [21]. Due to the lack of analytical variation propagation model for MAPs, the application of MPC in MAPs was limited since it requires a mathematical model to predict the final product quality with respect to the process adjustments. The development of state-space model has made it possible to implement the predictive MPC for the variation reduction in MAPs.

The objective of MPC for variation reduction in MAPs is to improve quality and minimize the variances of the KPC measurements, $\mathbf{y}_N$. Besides, the objective should also take into ac-

count the magnitudes of the control actions. Therefore, the performance of a control action at stage k, $\mathbf{u}_k$, can be evaluated by

$$\begin{aligned} J_k &= E\left[\hat{\mathbf{y}}_{N|k}^T \mathbf{Q}_N \hat{\mathbf{y}}_{N|k} + \mathbf{u}_k^T \mathbf{R}_k \mathbf{u}_k\right], \\ \text{s.t. } C_{k,c}^L &\le u_{k,c} \le C_{k,c}^U, \quad k = 1, \ldots, N, \\ c &= 1, \ldots, n_{u,k} \end{aligned} \tag{18}$$

where $\hat{\mathbf{y}}_{N|k}$ denotes the product quality at the final stage N that is predicted at stage k, and $n_{u,k}$ is the dimension of the control action $\mathbf{u}_k$. The constraints define the upper and lower PT actuation limits that can be applied on each part/subassembly. The control action limits, $C_{k,c}^L$ and $C_{k,c}^U$, are selected considering physical limitations of PTs workspace at each stage. This optimization index takes the form of the widely accepted cost function of a linear-quadratic regulator [22], and thus, satisfies the common requirements in control theory. The optimization index for determining the optimal control action is formulated as:

$$\begin{aligned} J_k^* &= \min_{\mathbf{u}_k} J_k = \min_{\mathbf{u}_k} E\left[\hat{\mathbf{y}}_{N|k}^T \mathbf{Q}_N \hat{\mathbf{y}}_{N|k} + \mathbf{u}_k^T \mathbf{R}_k \mathbf{u}_k\right], \\ \text{s.t. } C_{k,c}^L &\le u_{k,c} \le C_{k,c}^U, \quad k = 1, \ldots, N, \;\; c = 1, \ldots, n_{u,k} \end{aligned} \tag{19}$$

where $\mathbf{Q}_N$, $\mathbf{Q}_N \in \mathbf{R}^{m \times m}$, is assumed to be positive semi-definite, and $\mathbf{R}_k$, $\mathbf{R}_k \in \mathbf{R}^{n_{u,k} \times n_{u,k}}$, is a positive definite matrix.

B. Deviation of Optimal Control Action

In order to achieve J_k^*, the following assumptions are necessary:

A1) The expectation of an uncertainty matrix is assumed to be zero, e.g., $E\left[\tilde{\mathbf{B}}_k\right] = \mathbf{0}$, and the covariance between two uncertainty matrices are assumed known, e.g., $E\left[\tilde{\mathbf{B}}_k^T \tilde{\mathbf{B}}_k\right] = \Sigma_{\tilde{\mathbf{B}}_k}$. The latter covariance can be obtained from the theoretical derivation or the Monte Carlo simulation with given variation inputs. The expectation of higher order interactions are ignored.

A2) The expectations of unmodeled system errors and measurement noises are zero, i.e., $E[\mathbf{w}]_k = \mathbf{0}$ and $E[\mathbf{v}]_k = \mathbf{0}$, $k = 1, 2, \ldots, N$, and their covariance matrices are assumed known.

Under the above two assumptions, the optimal control actions, $\mathbf{u}_k$, that minimizes the performance index, J_k, can be obtained by solving $dJ_k/d\mathbf{u}_k = \mathbf{0}$. The solution to this optimization problem is

$$\begin{aligned} \mathbf{u}_k = -\Big(&\mathbf{\Gamma}_k^T \mathbf{Q}_N \mathbf{\Gamma}_k + E\left[\mathbf{\Gamma}_k^T \mathbf{Q}_N \tilde{\mathbf{\Gamma}}_k\right] \\ &+ E\left[\tilde{\mathbf{\Gamma}}_k^T \mathbf{Q}_N \mathbf{\Gamma}_k\right] + E\left[\tilde{\mathbf{\Gamma}}_k^T \mathbf{Q}_N \tilde{\mathbf{\Gamma}}_k\right] + \mathbf{R}_k\Big)^{-1} \\ \cdot \Big\{\Big(&\mathbf{\Gamma}_k^T \mathbf{Q}_N \mathbf{\Psi}_r + E\left[\tilde{\mathbf{\Gamma}}_k^T \mathbf{Q}_N \mathbf{\Psi}_r\right] + E\left[\mathbf{\Gamma}_k^T \mathbf{Q}_N \tilde{\mathbf{\Psi}}_r\right] \\ &+ E\left[\tilde{\mathbf{\Gamma}}_k^T \mathbf{Q}_N \tilde{\mathbf{\Psi}}_r\right]\Big) \hat{\mathbf{x}}_r\Big\} \end{aligned} \tag{20}$$

where the parameter matrices $\mathbf{\Gamma}_k$, $\tilde{\mathbf{\Gamma}}_k$, $\mathbf{\Psi}_r$ and $\tilde{\mathbf{\Psi}}_r$ are defined in (15) and (16). The detail derivation procedure is presented in Appendix I. The minimum is guaranteed by the positive-definite second-order derivative for an unconstrained objective function. The optimization is a convex optimization problem, and with the proposed type of constraints, the results will either be the optimal solution as given by the control law, or the solution on the constraint boundaries. This solution on boundaries is selected as the control action when the optimum obtained in (11) falls outside the feasible region, i.e.,

$$u_{k,c} = \begin{cases} u_{k,c}^* & \text{if } C_{k,c}^L < u_{k,c}^* < C_{k,c}^U \\ C_{k,c}^L \text{ or } C_{k,c}^U, & \text{if } u_{k,c}^* < C_{k,c}^L \text{ or } u_{k,c}^* > C_{k,c}^U \end{cases} \tag{21}$$

where $k = 1, \ldots, N$, $c = 1, \ldots, n_{u,k}$. The reason to include the second term with weighting matrix, $\mathbf{R}_k$, in the optimization index is to ensure the invertibility when calculating the control action with (20).

It is important to properly select the values of $\mathbf{Q}_N$ and $\mathbf{R}_k$. In most cases, $\mathbf{Q}_N$ and $\mathbf{R}_k$ are set to be diagonal matrices such that the first term in (19) is a weighted sum of squared elements in $\hat{\mathbf{y}}_N$, and the second term in (19) is a weighted sum of squared elements in $\mathbf{u}_k$, respectively. The values of elements in matrix $\mathbf{Q}_N$ are determined by the relative importance under the variation reduction purposes, with a larger value assigned to the $\mathbf{Q}_N$ element that corresponds to an important KPC. The selection of the relative magnitudes of elements in $\mathbf{Q}_N$ and $\mathbf{R}_k$ is difficult to make and may need trial and error simulations and tests. Different from the consideration of the stability and transient performances when selecting the weighting matrices for the LQG control problem [23], the selection of $\mathbf{Q}_N$ and $\mathbf{R}_k$ for this research is more related to the control performance in terms of the KPC variations at stage N. This is because that the transient performance is not a concern and the magnitudes of control actions have been constrained in the optimization set up (19). A rule of thumb to decide the values is to make the elements of $\mathbf{R}_k$ significantly smaller than that of $\mathbf{Q}_N$, but still keep $\mathbf{R}_k$ as a positive definite matrix. In this way, a significant variation reduction on $\mathbf{y}_N$ can be expected.

If model uncertainty is not considered, the model uncertainty terms can be ignored, and (20) will converge to $\mathbf{u}_k = -\left(\mathbf{\Gamma}_k^T \mathbf{Q}_N \mathbf{\Gamma}_k + \mathbf{R}_k\right)^{-1} \cdot \left(\mathbf{\Gamma}_k^T \mathbf{Q}_N \mathbf{\Psi}_r \hat{\mathbf{x}}_r\right)$. This is the same as the result derived using traditional optimal control, without considering model uncertainty.

The proposed control algorithm is generic to cover both 2-D panel-fitting assembly processes and 3-D general-assembly processes. With additional efforts in variation propagation modeling [24], [25], (19) can be used to derive the 3-D optimal control actions with consideration of model uncertainty.

IV. Case Study

A case study is conducted to illustrate the effectiveness of the control strategy developed in this paper. The case study is motivated by real industrial needs and manufacturing equipment capability. As documented in [8], in-line Optical Coordinate Measuring Machines have been widely adopted in automotive assembly processes. These devices can provide accurate in-line measurements of KPCs during production. At the same time, PTs have been used as fixture locators that can be adjusted on a part-to-part basis. Some study and test has been conducted in production environment to validate the concepts of active compensation with PTs for variation reduction. This case study further evaluates the control performance in variation reduction with considering model uncertainties.

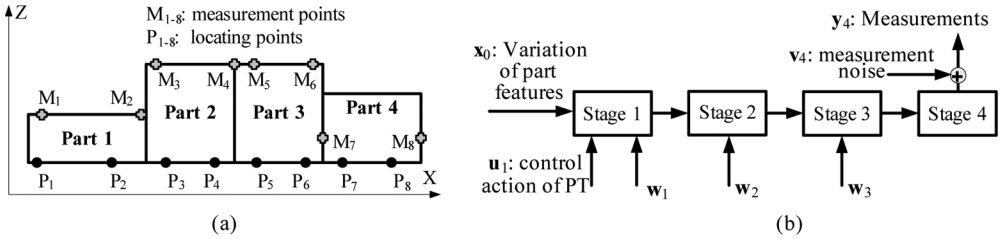

Fig. 3. Assembly process of the case study.

TABLE I
ASSEMBLY OPERATIONS AND LOCATING SCHEME

Stage Index	Operations	Locating Scheme 1		Locating Scheme 2		Output subassembly
		Part / subassembly	Locating points	Part / subassembly	Locating points	
1	Assembly	1	{P1, P2}	2	{P3, P4}	1&2
2	Assembly	1&2	{P1, P4}	3	{P5, P6}	1&2&3
3	Assembly	1&2&3	{P1, P6}	4	{P7, P8}	1&2&3&4
4	Measuring	1&2&3&4	{P1, P8}	\	\	\

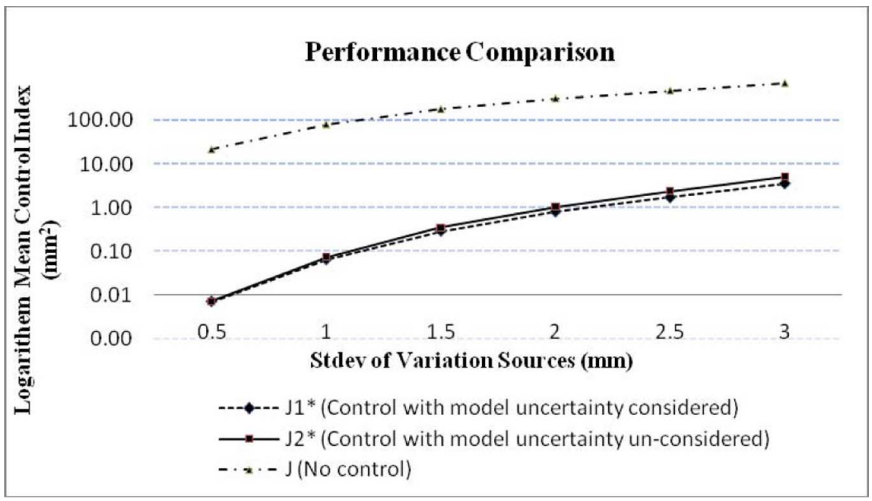

Fig. 4. Performance comparison for three control strategies.

The case study is conducted with a four-stage $(N = 4)$ assembly process that assembles four parts at three consecutive stages and measures the final product KPCs at the fourth stage, as illustrated in Fig. 3(a). The assembly operations, locating schemes and measuring strategy are summarized in Table I. For instance, in the first stage, part 1 and part 2 are located at points $\{P_1, P_2\}$ and $\{P_3, P_4\}$, respectively. These two parts are assembled to form subassembly 1&2. The final assembly, 1&2&3&4, is located at the 4th stage at points $\{P_1, P_8\}$ to collect the measurements on X-direction and Z-direction deviations of the eight points, $M_1 \sim M_8$. Thus, the number of quality variables contained in $\mathbf{y}_4$ is 16, i.e., $m = 16$. It is assumed that individual parts are measured before being located at the first stage. These measurements are used for calculating the optimal control actions performed by the controller installed in the first station, where the parts are assembled together after the control actions are carried out. The nominal product and process design information, represented as the nominal positions of the fixture locating pins and the measurement points, are summarized in Appendix II. Based on these predefined product and process information, the state-space model is derived, and the nominal system matrices are listed in Appendix III.

Dimensional variations are intentionally introduced to the locating points on Part 1 and Part 2, $P_1 \sim P_4$, to simulate the incoming variations from part features. It is assumed that their random deviations are normally distributed with zero means and nonzero variances. That is, the variations of the incoming part features are manifested as increase of variability, rather than the mean-shift. In order to ensure the delivery of quality product, PTs installed at stage 1 are used to adjust the positions of Part 1 and Part 2 and compensate their initial dimensional errors, as abstractly shown in Fig. 3(b).

In the case study, it is assumed that the model uncertainties are induced by dimensional variations of part features. Since the parts are generally fabricated according to the same tolerance allocation, it is assumed that the standard deviations of dimensional features of all the parts are the same. Thus, without loss of generality, a unique value, σ_I, has been set for all the features. Six model uncertainty conditions are studied by setting the σ_I at six different levels, i.e., $\sigma_I = 0.5$, $\sigma_I = 1$, $\sigma_I = 1.5$, $\sigma_I = 2$, $\sigma_I = 2.5$, and $\sigma_I = 3$, respectively. Correspondingly, the control actions denoted as $\mathbf{u}_1$ are taken to adjust the X-direction and the Z-direction positions of $P1 \sim P4$. Thus, the control action vector, u_1, is an 8×1 vector. The values of elements in

TABLE II
COMPARISON BETWEEN $J1^*$ AND $J2^*$ (SAMPLE SIZE: 1000)

σ_I		J1*	J2*	J	H_0: $\mu_{J1^*} = \mu_{J2^*}$ H_1: $\mu_{J1^*} < \mu_{J2^*}$	H_0: $\mu_{J2^*} = \mu_J$ H_1: $\mu_{J2^*} < \mu_J$
					p_value	p_value
0.5	Mean	0.0071	0.0072	21.8453	0.4115	**0.0000**
	Var	0.0001	0.0001	396.8163		
1	Mean	0.0651	0.0736	82.1999	**0.0398**	**0.0000**
	Var	0.0093	0.0142	0.6659×10^4		
1.5	Mean	0.2924	0.3515	184.7639	**0.0262**	**0.0000**
	Var	0.3174	0.6098	3.3281×10^4		
2	Mean	0.8069	1.0570	324.9011	**0.0013**	**0.0000**
	Var	2.1187	4.7700	1.1123×10^5		
2.5	Mean	1.7146	2.3879	489.3014	**0.00001**	**0.0000**
	Var	7.2696	17.8627	2.2094×10^5		
3	Mean	3.5600	5.1486	730.0909	**0.00004**	**0.0000**
	Var	47.0709	114.5761	4.7687×10^5		

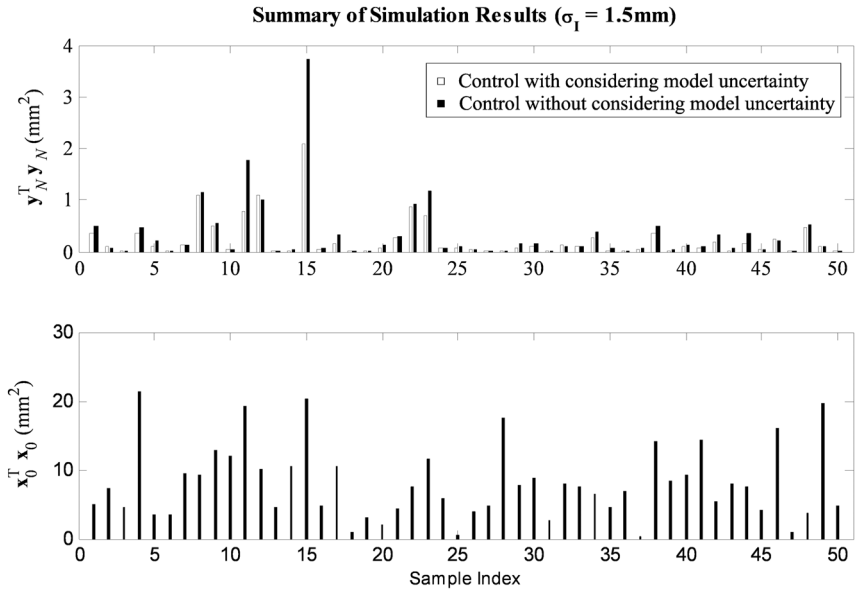

Fig. 5. Performance comparison of randomly selected 50 cars.

$\mathbf{u}_1$ are derived according to (20), with the random terms, such as $E(\hat{\mathbf{\Gamma}})$, obtained through Monte Carlo simulation with 1000 replications. Since all the PTs are provided by the same supplier, the constraints on all the elements in $\mathbf{u}_1$ are the same, i.e., $-10 \le u_{1,c} \le 10$, and $c = 1, 2, \ldots, 8$. Coefficient matrices, $\mathbf{Q}_4$ and $\mathbf{R}_1$, are $0.95{\cdot}\mathbf{I}_{16\times16}$ and $0.05{\cdot}\mathbf{I}_{8\times8}$, respectively. Three control strategies are considered, including *no control*, *control with model uncertainty considered*, and *control with model uncertainty unconsidered*. For all these three strategies, 1000 assembled products are generated with the same incoming variations, using Monte Carlo simulation. Their corresponding mean performances [as defined in (18)], J, $J1^*$, and $J2^*$, are estimated by the sample averages and their logarithm values are compared at different model uncertainty levels, as shown in Fig. 4.

It can be seen that the performances, in terms of the logarithm mean control index, of the processes with control ($J1^*$ and $J2^*$), are uniformly better than that of the process without control (J). In order to differentiate $J1^*$ and $J2^*$, the comparisons are also conducted by statistically testing the hypothesis H_0: $\mu_{J1^*} = \mu_{J2^*}$ versus H_1: $\mu_{J1^*} < \mu_{J2^*}$, under different σ_I. The sample mean and variance of the 1000 simulation replications corresponding to different σ_I's, as well as the hypothesis test results represented as the p-values are summarized in Table II. It is noted that when the variation of incoming part features are small, e.g., $\sigma_I = 0.5$, the model uncertainty level will be low and thus the performance difference between the two control strategies are *not* significant. When the incoming parts are with worse quality, which introduce more uncertainty to the state-space model, the performance of the control action derived with considering the model uncertainty, $J1^*$, will significantly outperform that derived without considering the model uncertainty, $J2^*$. Also tested are the hypotheses comparing the means of J and that of $J2^*$, i.e., H_0: $\mu_{J2^*} = \mu_J$ versus H_1: $\mu_{J2^*} < \mu_J$, under different σ_I. The hypotheses are uniformly rejected, indicating that the control actions are indeed necessary. This comparison verifies the effectiveness of the proposed control methodology.

Fifty simulation results are randomly selected from the 1000 simulated samples to illustrate the relationships between the incoming part quality, $\mathbf{x}_0^T\mathbf{x}_0$, and output quality, $\mathbf{y}_4^T\mathbf{y}_4$, as shown in Fig. 5. It can be seen that the feed-forward control without considering modeling error can generally reduce the impacts of

the incoming part variation on the final product. The proposed control can further reduce the impact that model uncertainty has on the controlled performance.

V. Conclusion

Random part fabrication and process induced errors will introduce uncertainties to the variation propagation models derived from the nominal product/process design of a MAP. A control methodology without considering such model uncertainty will result in a degradation of the controller performance in practice. A controller that is robust to model uncertainties is desirable. This paper proposes a mathematical MAP variation propagation model with considering the deviations of incoming parts and tooling features from their designed positions. For the first time, the optimal control actions are determined with explicit consideration of model uncertainties. Based on the proposed model, a predictive control strategy is derived with explicit consideration of model uncertainty. When the model uncertainty is significant, the control actions derived based on the proposed strategy will outperform the control without considering the model uncertainty. The effectiveness of the proposed approach is demonstrated through a case study of a simulated assembly processes.

Further investigations of the control for variation reduction in MAPs may be considered. As aforementioned, MRAC, H_∞ control, and fuzzy control are also potential methodologies to address this problem. Although the effectiveness of the feed-forward predictive control approach has been demonstrated in this paper, a comparison study of different methodologies, in terms of their effectiveness and efficiency, will be an interesting topic for both researchers and practitioners. In addition, the approach proposed in this paper is generic to rigid-body MAPs, and the application in compliant part manufacturing would be one of the promising future direction of this research. In order to deal with the control of MAP involving nonrigid parts/components, additional research efforts are needed to model variation propagation of nonrigid parts and further use them in the control applications.

Appendix I
Derivation of (19)

Denoted the prediction of $\mathbf{y}_N$ at stage k as $\hat{\mathbf{y}}_{N|k}$, which can be expanded in similar way as (17), i.e.,

$$\hat{\mathbf{y}}_{N|k} = \hat{\mathbf{\Gamma}}_k \mathbf{u}_k + \hat{\mathbf{\Psi}}_r \hat{\mathbf{x}}_r \tag{22}$$

where $\hat{\mathbf{\Gamma}}_i = \mathbf{C}_N \hat{\mathbf{A}}_{N-1} \dots \hat{\mathbf{A}}_i \hat{\mathbf{B}}_i = \mathbf{\Gamma}_i + \tilde{\mathbf{\Gamma}}_i$, $\hat{\mathbf{\Psi}}_i = \mathbf{C}_N \hat{\mathbf{A}}_{N-1} \dots \hat{\mathbf{A}}_i = \mathbf{\Psi}_i + \tilde{\mathbf{\Psi}}_i$, and stage r is an intermediate measurement stage. It can be easily observed that, $\tilde{\mathbf{\Gamma}}_i$ is a function of all $\mathbf{A}_j$'s, $\tilde{\mathbf{A}}_j$'s, $\mathbf{B}_j$'s and $\tilde{\mathbf{B}}_j$, $j = i, \dots, N-1$. Similarly, $\hat{\mathbf{\Psi}}_i = \mathbf{C}_N \hat{\mathbf{A}}_{N-1} \dots \hat{\mathbf{A}}_i = \mathbf{\Psi}_i + \tilde{\mathbf{\Psi}}_i$. Equation (22) can then be written as

$$\hat{\mathbf{y}}_{N|k} = \left(\mathbf{\Gamma}_k + \tilde{\mathbf{\Gamma}}_k\right) \mathbf{u}_k + \left(\mathbf{\Psi}_r + \tilde{\mathbf{\Psi}}_r\right) \hat{\mathbf{x}}_r + \sum_{i=r+1}^{N} \left(\mathbf{\Psi}_i + \tilde{\mathbf{\Psi}}_i\right) \mathbf{w}_i + \mathbf{v}_N. \tag{23}$$

Then, we can plug (23) into the expression of J_k

$$\begin{aligned} J_k &= E\left[\hat{\mathbf{y}}_{N|k}^T \mathbf{Q}_N \hat{\mathbf{y}}_{N|k} + \mathbf{u}_k^T \mathbf{R}_k \mathbf{u}_k\right] \\ &= E\Bigg\{ \mathbf{u}_k^T \mathbf{R}_k \mathbf{u}_k + \mathbf{u}_k^T \left(\mathbf{\Gamma}_k + \tilde{\mathbf{\Gamma}}_k\right)^T \mathbf{Q}_N \left(\mathbf{\Gamma}_k + \tilde{\mathbf{\Gamma}}_k\right) \mathbf{u}_k \\ &\quad + 2\mathbf{u}_k^T \left(\mathbf{\Gamma}_k + \tilde{\mathbf{\Gamma}}_k\right)^T \mathbf{Q}_N \Bigg[\left(\mathbf{\Psi}_r + \tilde{\mathbf{\Psi}}_r\right) \hat{\mathbf{x}}_r \\ &\quad + \sum_{i=r+1}^{N} \left(\mathbf{\Psi}_i + \tilde{\mathbf{\Psi}}_i\right) \mathbf{w}_i + \mathbf{v}_N \Bigg] \\ &\quad + \Bigg[\left(\mathbf{\Psi}_r + \tilde{\mathbf{\Psi}}_r\right) \hat{\mathbf{x}}_r \\ &\quad + \sum_{i=r+1}^{N} \left(\mathbf{\Psi}_i + \tilde{\mathbf{\Psi}}_i\right) \mathbf{w}_i + \mathbf{v}_N \Bigg]^T \mathbf{Q}_N \\ &\quad \cdot \Bigg[\left(\mathbf{\Psi}_r + \tilde{\mathbf{\Psi}}_r\right) \hat{\mathbf{x}}_r \\ &\quad + \sum_{i=r+1}^{N} \left(\mathbf{\Psi}_i + \tilde{\mathbf{\Psi}}_i\right) \mathbf{w}_i + \mathbf{v}_N \Bigg] \Bigg\}. \end{aligned} \tag{24}$$

The derivative of J_k with respect to $\mathbf{u}_k$ is

$$\begin{aligned} \frac{dJ_k}{d\mathbf{u}_k} &= E\Bigg[2\mathbf{R}_k \mathbf{u}_k + 2\left(\mathbf{\Gamma}_k + \tilde{\mathbf{\Gamma}}_k\right)^T \mathbf{Q}_N \left(\mathbf{\Gamma}_k + \tilde{\mathbf{\Gamma}}_k\right) \mathbf{u}_k \\ &\quad + 2\left(\mathbf{\Gamma}_k + \tilde{\mathbf{\Gamma}}_k\right)^T \mathbf{Q}_N \Bigg(\left(\mathbf{\Psi}_r + \tilde{\mathbf{\Psi}}_r\right) \hat{\mathbf{x}}_r \\ &\quad + \sum\nolimits_{i=r+1}^{N} \left(\mathbf{\Psi}_i + \tilde{\mathbf{\Psi}}_i\right) \mathbf{w}_i + \mathbf{v}_N \Bigg) \Bigg] \\ &= 2E\Bigg[\left(\left(\mathbf{\Gamma}_k + \tilde{\mathbf{\Gamma}}_k\right)^T \mathbf{Q}_N \left(\mathbf{\Gamma}_k + \tilde{\mathbf{\Gamma}}_k\right) + \mathbf{R}_k \right) \mathbf{u}_k \\ &\quad + \left(\mathbf{\Gamma}_k + \tilde{\mathbf{\Gamma}}_k\right)^T \mathbf{Q}_N \left(\mathbf{\Psi}_r + \tilde{\mathbf{\Psi}}_r\right) \hat{\mathbf{x}}_r \Bigg]. \end{aligned} \tag{25}$$

The two terms on the right-hand side of the above equation can be calculated as

$$\begin{aligned} &E\left[\left(\left(\mathbf{\Gamma}_k + \tilde{\mathbf{\Gamma}}_k\right)^T \mathbf{Q}_N \left(\mathbf{\Gamma}_k + \tilde{\mathbf{\Gamma}}_k\right) + \mathbf{R}_k \right) \mathbf{u}_k \right] \\ &= E\left[\mathbf{\Gamma}_k^T \mathbf{Q} \mathbf{\Gamma}_k + \mathbf{\Gamma}_k^T \mathbf{Q} \tilde{\mathbf{\Gamma}}_k + \tilde{\mathbf{\Gamma}}_k^T \mathbf{Q} \mathbf{\Gamma}_k + \tilde{\mathbf{\Gamma}}_k^T \mathbf{Q} \tilde{\mathbf{\Gamma}}_k + \mathbf{R}_k \right] \mathbf{u}_k \\ &= \Big(\mathbf{\Gamma}_k^T \mathbf{Q} \mathbf{\Gamma}_k + E\left[\mathbf{\Gamma}_k^T \mathbf{Q} \tilde{\mathbf{\Gamma}}_k\right] + E\left[\tilde{\mathbf{\Gamma}}_k^T \mathbf{Q} \mathbf{\Gamma}_k\right] \\ &\quad + E\left[\tilde{\mathbf{\Gamma}}_k^T \mathbf{Q} \tilde{\mathbf{\Gamma}}_k\right] + \mathbf{R}_k \Big) \mathbf{u}_k, \end{aligned}$$

and

$$\begin{aligned} &E\left[\left(\mathbf{\Gamma}_k + \tilde{\mathbf{\Gamma}}_k\right)^T \mathbf{Q}_N \left(\mathbf{\Psi}_r + \tilde{\mathbf{\Psi}}_r\right) \hat{\mathbf{x}}_r \right] \\ &= E\left[\mathbf{\Gamma}_k^T \mathbf{Q}_N \mathbf{\Psi}_r + \mathbf{\Gamma}_k^T \mathbf{Q}_N \tilde{\mathbf{\Psi}}_r \right. \\ &\quad \left. + \tilde{\mathbf{\Gamma}}_k^T \mathbf{Q}_N \mathbf{\Psi}_r + \tilde{\mathbf{\Gamma}}_k^T \mathbf{Q}_N \tilde{\mathbf{\Psi}}_r \right] \hat{\mathbf{x}}_r \\ &= \Big(\mathbf{\Gamma}_k^T \mathbf{Q}_N \mathbf{\Psi}_r + E\left[\mathbf{\Gamma}_k^T \mathbf{Q}_N \tilde{\mathbf{\Psi}}_r\right] + E\left[\tilde{\mathbf{\Gamma}}_k^T \mathbf{Q}_N \mathbf{\Psi}_r\right] \\ &\quad + E\left[\tilde{\mathbf{\Gamma}}_k^T \mathbf{Q}_N \tilde{\mathbf{\Psi}}_r\right] \Big) \hat{\mathbf{x}}_r. \end{aligned}$$

Set the derivative to $\mathbf{0}$, thus the suboptimal $\mathbf{u}_k$ can be obtained as

$$\begin{aligned}\mathbf{u}_k = &-\left(\mathbf{\Gamma}_k^T\mathbf{Q}_N\mathbf{\Gamma}_k + E\left[\mathbf{\Gamma}_k^T\mathbf{Q}_N\tilde{\mathbf{\Gamma}}_k\right]\right.\\ &\left.+E\left[\tilde{\mathbf{\Gamma}}_k^T\mathbf{Q}_N\mathbf{\Gamma}_k\right] + E\left[\tilde{\mathbf{\Gamma}}_k^T\mathbf{Q}_N\tilde{\mathbf{\Gamma}}_k\right] + \mathbf{R}_k\right)^{-1}\\ &\cdot\left(\left(\mathbf{\Gamma}_k^T\mathbf{Q}_N\mathbf{\Psi}_r + E\left[\tilde{\mathbf{\Gamma}}_k^T\mathbf{Q}_N\mathbf{\Psi}_r\right]\right.\right.\\ &\left.\left.+E\left[\mathbf{\Gamma}_k^T\mathbf{Q}_N\tilde{\mathbf{\Psi}}_r\right] + E\left[\tilde{\mathbf{\Gamma}}_k^T\mathbf{Q}_N\tilde{\mathbf{\Psi}}_r\right]\right)\hat{\mathbf{x}}_r\right).\end{aligned}$$

The above expression takes a common format of an optimal control action. The second derivate of J_k with respect to $\mathbf{u}_k$ is $E\left[\left(\mathbf{\Gamma}_k+\tilde{\mathbf{\Gamma}}_k\right)^T\mathbf{Q}\left(\mathbf{\Gamma}_k+\tilde{\mathbf{\Gamma}}_k\right)\right]+\mathbf{R}_k$, which is positive definite, and grantees that it is the optimal minimal point.

APPENDIX II

TABLE III
PRODUCT AND PROCESS DESIGN INFORMATION (UNIT: MM)

	Fixture Locating Pin Positions			Measurement Point Positions	
	X	Z		X	Z
P_1	100.0	100.0	M_1	200.0	400.0
P_2	150.0	100.0	M_2	700.0	400.0
P_3	800.0	100.0	M_3	700.0	600.0
P_4	850.0	100.0	M_4	1500.0	600.0
P_5	1500.0	100.0	M_5	1550.0	600.0
P_6	1550.0	100.0	M_6	2100.0	600.0
P_7	2300.0	100.0	M_7	2200.0	200.0
P_8	2350.0	100.0	M_8	2700.0	200.0

APPENDIX III

This appendix shows the system matrices of the state-space model for the case study shown at the bottom of this page and on the next page.

$$\mathbf{A}_1 = \left[\begin{array}{cccccc|c} 0 & 0 & 0 & 0 & 0 & 0 & \\ 0 & 0 & 0 & 0 & 0 & 0 & \\ 0 & 0.0013 & 1 & 0 & -0.0013 & -0.0667 & \\ -1 & 0 & 0 & 1 & 0 & 0 & \mathbf{\Theta}_{6\times6} \\ 0 & -0.0667 & 0 & 0 & 0.0667 & -46.6667 & \\ 0 & 0.0013 & 0 & 0 & -0.0013 & 0.9333 & \\ \hline \multicolumn{6}{c|}{\mathbf{\Theta}_{6\times6}} & \mathbf{I}_{6\times6} \end{array}\right]$$

$$\mathbf{A}_2 = \left[\begin{array}{ccccccccc|c} 0 & 0 & 0 & 0 & 0 & 0 & 0 & 0 & 0 & \\ 0 & 0 & 0 & 0 & 0 & 0 & 0 & 0 & 0 & \\ 0 & 0.0007 & 1 & 0 & 0 & 0 & 0 & -0.0007 & -0.0345 & \\ -1 & 0 & 0 & 1 & 0 & 0 & 0 & 0 & 0 & \\ 0 & -0.5172 & 0 & 0 & 1 & 0 & 0 & -0.4828 & -24.1379 & \mathbf{\Theta}_{9\times3} \\ 0 & 0.0007 & 0 & 0 & 0 & 1 & 0 & -0.0007 & -0.0345 & \\ -1 & 0 & 0 & 0 & 0 & 0 & 1 & 0 & 0 & \\ 0 & -0.0345 & 0 & 0 & 0 & 0 & 0 & 0.0345 & -48.2759 & \\ 0 & 0.0007 & 0 & 0 & 0 & 0 & 0 & -0.0007 & 0.9655 & \\ \hline \multicolumn{9}{c|}{\mathbf{\Theta}_{3\times9}} & \mathbf{I}_{3\times9} \end{array}\right]$$

$$\mathbf{A}_3 = \left[\begin{array}{ccc|c|ccc} 0 & 0 & 0 & & 0 & 0 & 0 \\ 0 & 0 & 0 & \mathbf{\Theta}_{3\times6} & 0 & 0 & 0 \\ 0 & 0.0004 & 1 & & 0 & -0.0004 & 0.0222 \\ \hline -1 & 0 & 0 & & 0 & 0 & 0 \\ 0 & -0.6889 & 0 & & 0 & -0.3111 & -15.5556 \\ 0 & 0.0004 & 0 & \mathbf{I}_{6\times6} & 0 & -0.0004 & -0.0222 \\ -1 & 0 & 0 & & 0 & 0 & 0 \\ 0 & -0.3778 & 0 & & 0 & -0.6222 & -31.1111 \\ 0 & 0.0004 & 0 & & 0 & -0.0004 & -0.0222 \\ \hline -1 & 0 & 0 & & 1 & 0 & 0 \\ 0 & -0.0222 & 0 & \mathbf{\Theta}_{3\times6} & 0 & 0.0222 & -48.8889 \\ 0 & 0.0004 & 0 & & 0 & -0.0004 & 0.9778 \end{array}\right]$$

$$\mathbf{B}_1 = \left[\begin{array}{cccc|cccc} 1 & 0 & 0 & 0 & \multicolumn{4}{c}{\multirow{4}{*}{$\mathbf{I}_{3\times 4}$}} \\ 0 & 1 & 0 & 0 & & & & \\ 0 & -0.02 & 0 & 0.02 & & & & \\ \hline \multicolumn{4}{c|}{\multirow{4}{*}{$\mathbf{I}_{3\times 4}$}} & 1 & 0 & 0 & 0 \\ & & & & 0 & 1 & 0 & 0 \\ & & & & 0 & -0.02 & 0 & 0.02 \\ \hline \multicolumn{8}{c}{$\mathbf{\Theta}_{6\times 8}$} \end{array}\right]$$

$$\mathbf{B}_2 = \left[\begin{array}{cccc|cccc} 1 & 0 & 0 & 0 & \multicolumn{4}{c}{\multirow{5}{*}{$\mathbf{\Theta}_{6\times 4}$}} \\ 0 & 1 & 0 & 0 & & & & \\ 0 & -0.0013 & 0 & 0.0013 & & & & \\ 1 & 0 & 0 & 0 & & & & \\ 0 & 0.0667 & 0 & 0.9333 & & & & \\ 0 & -0.0013 & 0 & 0.0013 & & & & \\ \hline \multicolumn{4}{c|}{\multirow{5}{*}{$\mathbf{\Theta}_{6\times 4}$}} & 1 & 0 & 0 & 0 \\ & & & & 0 & 1 & 0 & 0 \\ & & & & 0 & -0.02 & 0 & 0.02 \\ \hline \multicolumn{8}{c}{$\mathbf{\Theta}_{3\times 4}$} \end{array}\right]$$

$$\mathbf{B}_3 = \left[\begin{array}{cccc|cccc} 1 & 0 & 0 & 0 & \multicolumn{4}{c}{\multirow{8}{*}{$\mathbf{\Theta}_{9\times 4}$}} \\ 0 & 1 & 0 & 0 & & & & \\ 0 & -0.0007 & 0 & 0.0007 & & & & \\ 1 & 0 & 0 & 0 & & & & \\ 0 & 0.5172 & 0 & 0.4828 & & & & \\ 0 & -0.0007 & 0 & 0.0007 & & & & \\ 1 & 0 & 0 & 0 & & & & \\ 0 & 0.0345 & 0 & 0.9655 & & & & \\ 0 & -0.0007 & 0 & 0.0007 & & & & \\ \hline \multicolumn{4}{c|}{\multirow{4}{*}{$\mathbf{\Theta}_{3\times 4}$}} & 1 & 0 & 0 & 0 \\ & & & & 0 & 1 & 0 & 0 \\ & & & & 0 & -0.02 & 0 & 0.02 \end{array}\right]$$

$$\mathbf{C}_4 = \left[\begin{array}{ccc|ccc|ccc} 1 & 0 & -300 & \multicolumn{3}{c|}{\multirow{4}{*}{$\mathbf{\Theta}_{4\times 3}$}} & \multicolumn{3}{c}{\multirow{4}{*}{$\mathbf{\Theta}_{8\times 6}$}} \\ 0 & 1 & 100 & & & & & & \\ 1 & 0 & -300 & & & & & & \\ 0 & 1 & 600 & & & & & & \\ \hline \multicolumn{3}{c|}{\multirow{4}{*}{$\mathbf{\Theta}_{4\times 3}$}} & 1 & 0 & -500 & \multicolumn{3}{c}{} \\ & & & 0 & 1 & -100 & \multicolumn{3}{c}{} \\ & & & 1 & 0 & -500 & \multicolumn{3}{c}{} \\ & & & 0 & 1 & 700 & \multicolumn{3}{c}{} \\ \hline \multicolumn{6}{c|}{\multirow{4}{*}{$\mathbf{\Theta}_{8\times 6}$}} & 1 & 0 & -500 \\ & & & & & & 0 & 1 & 50 \\ & & & & & & 1 & 0 & -500 \\ & & & & & & 0 & 1 & 600 \\ \hline \multicolumn{6}{c|}{\multirow{4}{*}{$\mathbf{\Theta}_{4\times 3}$}} & 1 & 0 & -100 \\ & & & & & & 0 & 1 & -100 \\ & & & & & & 1 & 0 & -100 \\ & & & & & & 0 & 1 & 400 \end{array}\right]$$

ACKNOWLEDGMENT

The authors would like to thank for reviewers' and editor's comments that have helped us significantly improve this paper presentation.

REFERENCES

[1] W. Cai, "Robust pin layout design for sheet-panel locating," *Int. J. Advanced Manuf. Technol.*, vol. 28, no. 5–6, pp. 486–94, 2006.
[2] R. Mantripragada and D. E. Whitney, "Modeling and controlling variation propagation in mechanical assemblies using state transition models," *IEEE Trans. Robot. Autom.*, vol. 15, pp. 124–40, 1999.
[3] J. S. Fenner, M. K. Jeong, and L. Jye-Chyi, "Optimal automatic control of multistage production processes," *IEEE Trans. Semiconductor Manuf.*, vol. 18, pp. 94–103, 2005.
[4] S. Hu, "Impact of 100% measurement data on statistical process control (SPC) in automobile body assembly," Ph.D. dissertation, Univ. Michigan, Ann Arbor, MI, 1990.
[5] S. J. Hu and S. M. Wu, "Identifying root cause of variation in automobile body assembly using principal component analysis," *Trans. NAMRI*, vol. XX, pp. 311–316, 1992.
[6] D. Djurdjanovic and J. Ni, "On-Line stochastic control of dimensional quality in multi-station manufacturing systems," *J. Eng. Manuf., Proc. Institution of Mechanical Engineers*, vol. 207, no. 5, pp. 865–880, 2007.
[7] D. Djurdjanovic and J. Zhu, "Stream of variation model based compensation of dimensional errors in multistage manufacturing," in *Proc. ASME Int. Mech. Eng. Congr. Expo., IMECE*, 2005, Paper No. IMECE2005-81550.
[8] L. E. Izquierdo, J. Shi, S. J. Hu, and C. W. Wampler, "Feedforward control of multistage assembly processes using programmable tooling," *Trans. NAMRI/SME*, vol. 35, pp. 295–302, 2007.
[9] J. Zhong, "Manufacturing system variation reduction through feedforward control considering model uncertainties," Ph.D. dissertation, Univ. Michigan, Ann Arbor, MI, 2009.
[10] K. J. Astrom, "Adaptive control around 1960," *IEEE Control Syst. Mag.*, vol. 16, no. 3, pp. 44–9, 1996.
[11] T. Basar and P. Bernhard, *H-Infinity Optimal Control and Related Minimax Design Problems: A Dynamic Game Approach*, 2nd ed. Boston, MA: Birkhäuser, 1995.
[12] H. Kwakernaak, "H_2-optimization—Theory and applications to robust control design," *Annu. Reviews in Control*, vol. 26, no. 1, pp. 45–56, 2005.
[13] K. Tanaka and M. Sugeno, "Stability analysis and design of fuzzy control systems," *Fuzzy Sets and Systems*, vol. 45, no. 2, pp. 135–156, 1992.
[14] J. Jin and J. Shi, "State space modeling of sheet metal assembly for dimensional control," *ASME Trans., J. Manuf. Sci. Eng.*, vol. 121, pp. 756–762, 1999.
[15] J. Shi, *Stream of Variation Modeling and Analysis for Multistage Manufacturing Processes*. Boca Raton, FL: CRC Press, 2006, ISBN: 0-8493-2151-4.
[16] Y. Ding, D. D. Ceglarek, and J. Shi, "Modeling and diagnosis of multistation manufacturing processes: State space model," in *Proc. 2000 Japan/USA Symp. Flexible Automation*, 2000.
[17] Low-Volume Vehicle Production Manufacturing, Engineering, and Technology Group, Center for Automotive Research, Tech. Rep., 2006.
[18] J. M. Maciejowski, *Predictive Control: With Constraints*. Harlow, New York: Prentice Hall, 2002.
[19] S. J. Qin and T. A. Badgwell, "A survey of industrial model predictive control technology," *Control Engineering Practice*, vol. 11, no. 7, pp. 733–64, 2003.
[20] J. H. Lee and B. Cooley, "Recent advances in model predictive control and other related areas," in *Proc. 5th Int. Conf. Chem. Process Control: AICHE Symp.*, 1997.
[21] S. D. Cairano, A. Bemporad, I. Kolmanovsky, and D. Hrovat, "Model predictive control of magnetic automotive actuators," in *Proc. Amer. Control Conf.*, Piscataway, NJ, 2007, pp. 5082–5087.
[22] K. E. Donald, *Optimal Control Theory: An Introduction*. Englewood Cliffs, NJ: Prentice-Hall, 1970, pp. 452–452.
[23] K. J. Astrom and B. Wittenmark, *Computer Controlled Systems: Theory and Design*. Englewood Cliffs, NJ: Prentice-Hall, 1984, pp. 430–430.
[24] J. Liu, J. Jin, and J. Shi, Development of a CAE design tool for minimizing door seal gap variation by optimizing component and sub-assembly locator position & orientation Univ. Michigan, Ann Arbor, MI, Tech. Rep., 2008.
[25] J. Liu, J. Jin, and J. Shi, "State space modeling for 3-dimensional variation propagation in rigid-body multistage assembly processes," *IEEE Trans. Autom. Sci. Eng.*, 2009, in press.

Jing Zhong received the B.S. degree in electronic engineering from the Tsinghua University, Beijing, China, in 2003, the M.A. degree in statistics, the M.S. degree in industrial engineering, and the Ph.D. degree in industrial and operations engineering, all from the University of Michigan, Ann Arbor, in 2006, 2007 and 2009, respectively.

Currently, she is working with the Microsoft Corporation, Bellevue, WA. Her research interests are focused on high-dimensional data mining and engineering statistics.

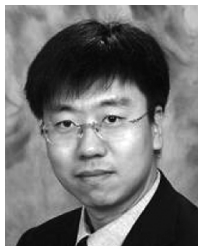

Jian Liu received the B.S. and M.S. degrees in precision instruments and mechanology from the Tsinghua University, Beijing, China, in 1999 and 2002, respectively, the M.S. degree in industrial engineering, the M.S. degree in statistics, and the Ph.D. degree in mechanical engineering and industrial engineering, all from the University of Michigan, Ann Arbor, in 2005, 2006, and 2008, respectively.

Currently, he is an Assistant Professor in the Department of Systems and Industrial Engineering, University of Arizona, Tucson. His research is centered on the integration of manufacturing engineering knowledge, control theory and advanced statistics for product quality and productivity improvement.

Prof. Liu is a member of The Institute for Operations Research and the Management Sciences (INFORMS) and the Institute of Industrial Engineers (IIE).

Jianjun Shi received the B.S. and M.S. degrees in electrical engineering from the Beijing Institute of Technology, Beijing, China, in 1984 and 1987, respectively, and the Ph.D. degree in mechanical engineering from the University of Michigan, Ann Arbor, in 1992.

Currently, he is the Carolyn J. Stewart Chair Professor in the H. Milton Stewart School of Industrial and Systems Engineering, Georgia Institute of Technology, Atlanta. His research interests include the fusion of advanced statistical and domain knowledge to develop methodologies for modeling, monitoring, diagnosis, and control for complex manufacturing systems.

Dr. Shi is a Fellow of the Institute of Industrial Engineers (IIE), a Fellow of American Society of Mechanical Engineers (ASME), a Fellow of The Institute for Operations Research and the Management Sciences (INFORMS), and a member of ASQ, SME, and ASA.